Research Article

Approximate Analytical Three-Dimensional Multiple Time Scales Solution to a Circular Restricted Three-Body Problem

Fabao Gao [ID] **and Yongqing Wang**

School of Mathematical Science, Yangzhou University, Yangzhou 225002, China

Correspondence should be addressed to Fabao Gao; gaofabao@sina.com

We illustrate the chaotic nature of the circular restricted three-body problem from the perspective of the bifurcation diagram with respect to the mass ratio parameter. Moreover, it is shown that when the frequency ratio in different directions of the classical problem is irrational, it has the quasiperiodic characteristics. In addition, a three-dimensional approximate solution to this problem under two time scales is proposed by using the multiple time scales method.

1. Introduction

As early as the 19th century, plenty of mathematicians, such as Dirichlet and Weierstrass, et al. [1], expected to obtain a series solution of the three-body problem in the following form:

$$\sum_{j=1}^{\infty} \left[A_j \cos\left(\sum_{i=1}^{k} (j_i \omega_i) \right) t + B_j \sin\left(\sum_{i=1}^{k} (j_i \omega_i) \right) t \right]. \quad (1)$$

The rate of change of the solution with respect to time t in equation (1) appears as a combination of many incommensurable frequencies, $\omega_i i = 1, 2, \ldots, k$, often called quasiperiodic solution.

Almost half a century ago, Farquhar and Kamel [2] proposed an approximation to construct the periodic orbits described above. A few years later, Richardson [3, 4] developed third-order analytic solutions to collinear libration points (CLP) for a class of circular restricted three-body problem (CRTBP) based on a method similar to Lindstedt–Poincaré and successive approximation. The constructed solutions are the basis of determining halo orbits around these points, and they can provide approximate initial values of halo orbits. Furthermore, the solutions

can also be developed to investigate spacecraft formation flying. The more accurate the approximate analytical solutions, the less fuel in the system will be consumed. Ruijgrok [5] solved a planar three-body problem for equal mass particles under a particular class of three-body forces. Zagouras and Markellos [6] studied a periodic spatial solution to Hill's problem, which is the limiting case of a restricted three-body problem (R3BP). Papadakis et al. [7] considered the periodic orbits of the three-body problem generated by CLP and provided the second-order approximate analytic expressions of such orbits. Gómez et al. [8] computed quasihalo orbits in CRTBP semianalytically through the Lindstedt–Poincaré technique. Ten years ago, Lu and Zhao [9] proposed an improved and more precise third-order analytic solution than Richardson's classical analytic solution. Gidea and Deppe [10] numerically studied the influence of small perturbations on the dynamics of an infinitesimal third body. They investigated the chaotic orbits in an RTBP, which also indicated the complexity and difficulty of obtaining approximate analytic solutions to the problem.

In recent years, Šuvakov and Dmitrašinovic [11] presented some creative results for the periodic orbits of the three-body problem. Thirteen new, zero-angular-

momentum, distinct equal mass, planar collisionless periodic orbits are displayed in three new categories. When the two primaries are both oblate spheres, Mittal et al. [12] used the predictor-corrector algorithm to construct periodic orbits. They showed the corresponding periodic orbits under different energy constants, mass ratios, and oblateness factors of the two primaries. Based on photogravitational planar RTBP with oblateness, Pathak et al. [13] studied the seventh-, ninth-, and eleventh-order internal resonance periodic orbits of the Sun-Earth system by using Runge–Kutta–Gill method. For a generalized photogravitational RTBP model, the two primaries are oblate spheroid and are under the gravity of an asteroid belt. Abouelmagd et al. [14] found a secular solution that can be reduced to a periodic one near the triangular libration points when the mass ratio is equal to the critical mass value. Similar results can also be found in [15]. Selim et al. [16] analyzed the stable motion solutions of long-period orbits and short-period orbits when the primary is a triaxial rigid body and the Euler angle of rotation satisfies certain conditions. Besides, for two types of the perturbed RTBP, Gao et al. [17, 18] utilized the Lindstedt–Poincaré perturbation method to give an approximate analytical solution to the periodic orbits near the CLP.

Considering that the dynamical equation of the third body in CR3BP is a time-varying high-dimensional nonlinear system in the inertial frame, it can hardly be solved by using analytical approaches. However, this case will be better in the rotating coordinate system, for the aforementioned governing equations are time-independent, and there is an integrable motion. Using the method of multiple time scales, Nayfeh [19, 20] studied the $3:1$ and $2:1$ small-amplitude resonances near the triangular libration points in the plane when the potential function was expanded to the second- and third-order terms of a small parameter, respectively.

Based on the number of terms expanded by the potential function of the problem, the existing time-scale solutions mainly include the three-dimensional single time-scale solution when the potential function expands to the third-order, the three-dimensional (3D) double time-scale solution when the potential function expands to the second-order, and the planar approximate analytic solution. Accordingly, when the third body is also considered to vibrate with a small amplitude in space, the multiple time scales method [21] will be used to construct the approximate 3D CR3BP solution in this paper. The 3D multiple time scales solution has the following form:

$$\mathbf{u} = \sum_{l=1}^{2} \varepsilon^l \mathbf{u}_l (t, \varepsilon t), \qquad (2)$$

where $\mathbf{u} = (x, y, z)$, $\mathbf{u}_l = (x_1, y_1, z_1)$, $l = 1, 2$, and ε is a small, dimensionless parameter.

2. Dynamic Equations of Classical CRTBP

In this section, the dynamic equations of classical CRTBP in three-dimensional space will be described.

In a rotating framework, it is well known that the governing equations of the classical CRTBP can be characterized by the following set of differential equations:

$$\ddot{x} - 2\dot{y} = x - U_x, \quad \ddot{y} + 2\dot{x} = y - U_y, \qquad \ddot{z} = -U_Z, \qquad (3)$$

where the potential function

$$U(x, y, z) = -\frac{1 - \mu}{\left[(x + \mu)^2 + y^2 + z^2 \right]^{(1/2)}} \\ - \frac{\mu}{\left[(x - 1 + \mu)^2 + y^2 + z^2 \right]^{(1/2)}}. \qquad (4)$$

For more details on the establishment of equation (3), please refer to [22].

It is easy to find that μ in equation (4) is the only parameter in the classical CRTBP. In this paper, we define it as the ratio of the mass of one primary to the mass sum of the two primaries, so it is called the mass ratio parameter, and its value range is between 0 and 1. Under the initial conditions $[-0.001, 0.2, 0.1, -0.3, 0.87, 0.01]$, we divide the range of μ into 1000 equal parts, and then, respectively, return its corresponding coordinates of three different planes (x-y, x-z, y-z) for each value of μ, and the bifurcation diagram with respect to the parameter μ based on ode45 algorithm shows that any small change of μ will lead to the third body's apparent chaotic dynamic behavior (see Figure 1). We find that any value of μ corresponds to an infinite number of points rather than a single point, which means that the probability of obtaining periodic solutions of the three-body problem by numerical simulation is almost zero. Moreover, even if there are some results that are seem to be periodic, part of the existing conclusions based on numerical simulation will no longer hold when the step size continues to shrink. When the iteration accuracy is gradually improved, it is difficult for the orbit of the three-body system with chaotic characteristics to come back after iteration from a particular initial point, and researchers do not even know what will happen when the accuracy is less than 10^{-16}. Therefore, we expect that the periodic solution which is beneficial to the actual mission can be realized by "construction."

Next, we first deal with the complex potential function $U(x, y, z)$ by introducing Legendre polynomials P_n, which satisfies Rodrigues formula:

$$P_n(x) = \frac{1}{2^n n!} \frac{d^n}{dx^n} \left(x^2 - 1 \right)^n, \quad n = 0, 1, 2, 3, \ldots. \qquad (5)$$

Then, we have [22]

(a)

(b)

(c)
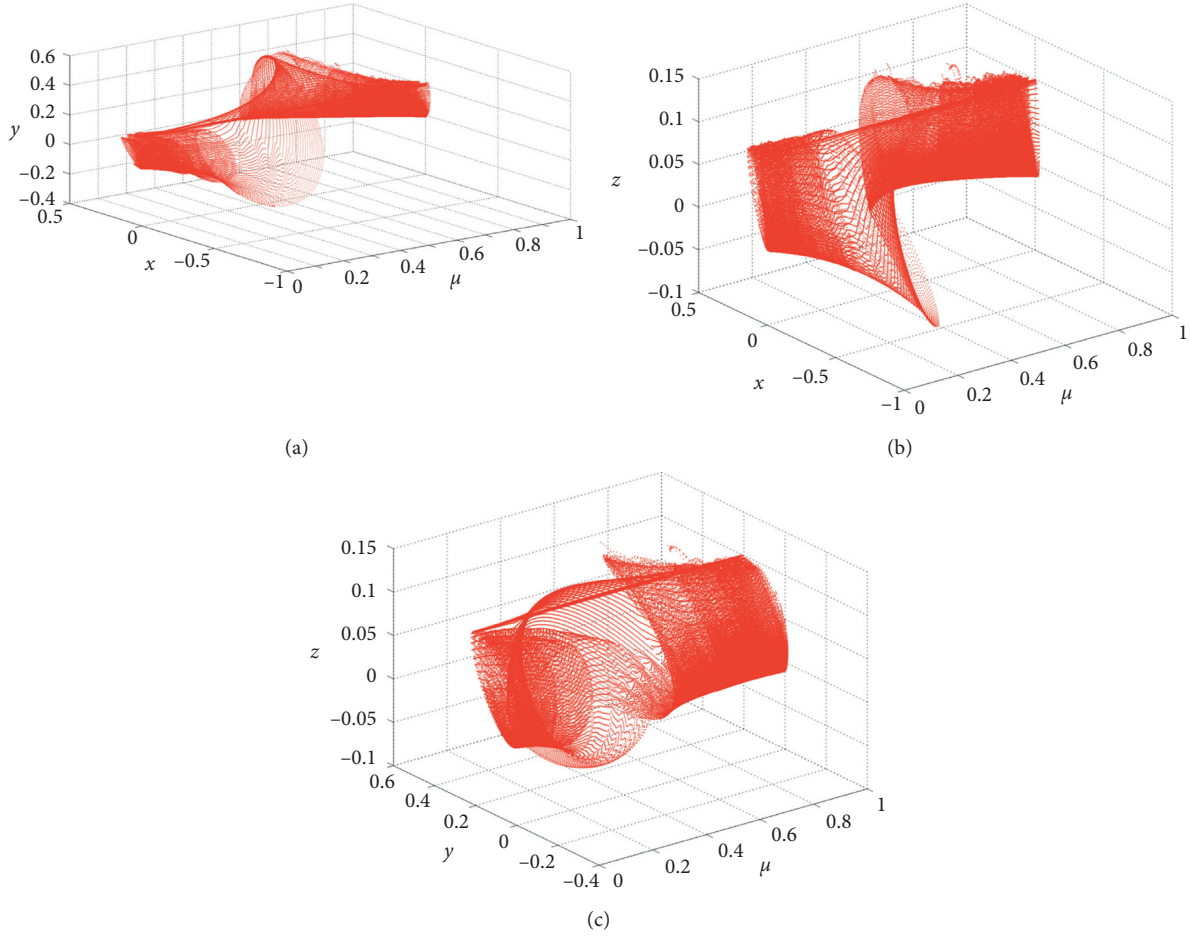
FIGURE 1: (a–c) Bifurcation diagrams of mass ratio parameters in μ-x-y, μ-x-z, and μ-y-z frames, respectively.

$$\frac{1}{\left[(x-A)^2 + (y-B)^2 + (z-C)^2\right]^{(1/2)}} = \frac{1}{D} \sum_{n=0}^{\infty} \left(\frac{\rho}{D}\right)^n P_n\left(\frac{Ax + By + Cz}{D\rho}\right), \tag{6}$$

where $D^2 = A^2 + B^2 + C^2$ and $\rho = x^2 + y^2 + z^2$.

Substituting equations (4) and (6) into equation (3), it yields

$$\ddot{x} - 2\dot{y} - (1 + 2c_2)x = \frac{\partial}{\partial x} \sum_{n \geq 3} c_n \rho^n P_n\left(\frac{x}{\rho}\right), \qquad \ddot{y} + 2\dot{x} + (c_2 - 1)y = \frac{\partial}{\partial y} \sum_{n \geq 3} c_n \rho^n P_n\left(\frac{x}{\rho}\right), \ddot{z} + c_2 z = \frac{\partial}{\partial z} \sum_{n \geq 3} c_n \rho^n P_n\left(\frac{x}{\rho}\right), \tag{7}$$

where
$c_n = (1/\gamma_L^3)[(\pm 1)^n \mu + (-1)^n((1-\mu)\gamma_L^{n+1}/(1\mp\gamma_L)^{n+1})]$, for libration points L_1 and L_2 and $c_n = (1/\gamma_L^3)$ $[1 - \mu + (\mu\gamma_L^{n+1}/(1 + \gamma_L)^{n+1})]$, for libration point L_3,

$\gamma_L = n_1^{(2/3)}$, where n_1 represents the angular velocity of relative motion between the two primaries.

Then, equation (7), up to the third approximation, can be written in the following form:

$$\ddot{x} - 2\dot{y} - (1 + 2c_2)x = \frac{3}{2}c_3(2x^2 - y^2 - z^2) + 2c_4(2x^2 - 3y^2 - 3z^2), \qquad + 2\dot{x} + (c_2 - 1)y = -3c_3xy - \frac{3}{2}c_4y(4x^2 - y^2 - z^2), \ddot{z}$$

$$\ddot{y}$$

$$+ c_2z$$

$$= -3c_3xz - \frac{3}{2}c_4z(4x^2 - y^2 - z^2).$$

$$(8)$$

3. Construction of Approximate 3D Multiple Time Scales Solution

Consider the small amplitude of nonhomogeneous terms of equation (8). Then,

$$\ddot{x} - 2\dot{y} - (1 + 2c_2)x = \frac{3}{2}\varepsilon c_3(2x^2 - y^2 - z^2) + 2\varepsilon c_4(2x^2 - 3y^2 - 3z^2), \qquad + 2\dot{x} + (c_2 - 1)y = -3\varepsilon c_3xy - \frac{3}{2}\varepsilon c_4y(4x^2 - y^2 - z^2), \ddot{z}$$

$$\ddot{y}$$

$$+ c_2z$$

$$= -3\varepsilon c_3xz - \frac{3}{2}\varepsilon c_4z(4x^2 - y^2 - z^2).$$

$$(9)$$

We write the solution of equation (9) as follows:

$$x = \sum_{l=1}^{2} \varepsilon^l x_l(T_0, T_1),$$

$$y = \sum_{l=1}^{2} \varepsilon^l y_l(T_0, T_1), \qquad (10)$$

$$z = \sum_{l=1}^{2} \varepsilon^l z_l(T_0, T_1),$$

where $T_0 = t$ and $T_1 = \varepsilon t$.

Then, time derivatives become

$$\frac{d}{dt} = \frac{\partial}{\partial T_0}\frac{dT_0}{dt} + \frac{\partial}{\partial T_1}\frac{dT_1}{dt} + \cdots = D_0 + \varepsilon D_1 + \cdots, \quad (11)$$

$$\frac{d^2}{dt^2} = (D_0 + \varepsilon D_1 + \cdots)^2 = D_0^2 + 2\varepsilon D_0 D_1 + \cdots, \quad (12)$$

where $D_k = (\partial/\partial T_k)$, $k = 0, 1, \ldots$

Substituting equations (10)–(12) into equation (9), we find

$$\left[D_0^2 x_1 - 2D_0 y_1 - (1 + 2c_2)x_1\right]\varepsilon + \left[D_0^2 x_2 + 2D_0 D_1 x_1 - 2D_0 y_2 - 2D_1 y_1 - (1 + 2c_2)x_2\right]\varepsilon^2 + 2(D_0 D_1 x_2 - D_1 y_2)\varepsilon^3$$

$$(13a)$$

$$= \frac{3}{2}c_3(2x_1^2 - y_1^2 - z_1^2)\varepsilon^3 + \left[2c_4(2x_1^2 - 3y_1^2 - 3z_1^2)x_1 + 3c_3(2x_1 x_2 - y_1 y_2 - z_1 z_2)\right]\varepsilon^4 + O(\varepsilon^5),$$

$$\left[D_0^2 y_1 + 2D_0 x_1 + (c_2 - 1)y_1\right]\varepsilon + \left[D_0^2 y_2 + 2D_0 D_1 y_1 + 2D_0 x_2 + 2D_1 x_1 + (c_2 - 1)y_2\right]\varepsilon^2 + 2(D_0 D_1 y_2 + D_1 x_2)\varepsilon^3$$

$$(13b)$$

$$= -3c_3 x_1 y_1 \varepsilon^3 - 3\left[c_3(x_1 y_2 + x_2 y_1) + \frac{1}{2}c_4(4x_1^2 - y_1^2 - z_1^2)y_1\right]\varepsilon^4 + O(\varepsilon^5),$$

$$\left(D_0^2 z_1 + c_2 z_1\right)\varepsilon + \left(D_0^2 z_2 + 2D_0 D_1 z_1 + c_2 z_2\right)\varepsilon^2 + 2D_0 D_1 z_2 \varepsilon^3$$

$$(13c)$$

$$= -3c_3 x_1 z_1 \varepsilon^3 - 3\left[c_3(x_1 z_2 + x_2 z_1) + \frac{1}{2}c_4(4x_1^2 - y_1^2 - z_1^2)z_1\right]\varepsilon^4 + O(\varepsilon^5).$$

Now, from equations (13a)–(13c), equating the coefficients of ε, ε^2, and ε^3 to zero, it leads to the following three sets of equations.

Order ε:

$$D_0^2 x_1 - 2D_0 y_1 - (1 + 2c_2) x_1 = 0,$$
$$D_0^2 y_1 + 2D_0 x_1 + (c_2 - 1) y_1 = 0, \qquad (14)$$
$$D_0^2 z_1 + c_2 z_1 = 0.$$

Order ε^2:

$$D_0^2 x_2 + 2D_0 D_1 x_1 - 2D_0 y_2 - 2D_1 y_1 - (1 + 2c_2) x_2 = 0,$$
$$D_0^2 y_2 + 2D_0 D_1 y_1 + 2D_0 x_2 + 2D_1 x_1 + (c_2 - 1) y_2 = 0,$$
$$D_0^2 z_2 + 2D_0 D_1 z_1 + c_2 z_2 = 0.$$
$$(15)$$

Order ε^3:

$$2D_0 D_1 x_2 - 2D_1 y_2 = \frac{3}{2} c_3 \left(2x_1^2 - y_1^2 - z_1^2 \right),$$
$$2D_0 D_1 y_2 + 2D_1 x_2 = -3c_3 x_1 y_1, \qquad (16)$$
$$2D_0 D_1 z_2 = -3c_3 x_1 z_1.$$

Consider that the last equation of (14) is decoupled from the first two equations of (14). We employ the following transformations:

$$x_1 = \omega_1,$$
$$\dot{\omega}_1 = \omega_2,$$
$$y_1 = \omega_3, \qquad (17)$$
$$\dot{\omega}_3 = \omega_4.$$

Then, the first two equations of (14) can be represented by the following equivalent form:

$$\dot{\omega}_1 = \omega_2,$$
$$\dot{\omega}_2 = (1 + 2c_2) \omega_1 + 2\omega_4,$$
$$\dot{\omega}_3 = \omega_4, \qquad (18)$$
$$\dot{\omega}_4 = -2\omega_2 + (1 - c_2) \omega_3.$$

Thus, the coefficient matrix of equation (18) can be denoted as

$$\begin{bmatrix} 0 & 1 & 0 & 0 \\ 1 + 2c_2 & 0 & 0 & 2 \\ 0 & 0 & 0 & 1 \\ 0 & -2 & 1 - c_2 & 0 \end{bmatrix}. \qquad (19)$$

Therefore, the characteristic equation can be obtained as

$$\widehat{\lambda}^4 + (2 - c_2) \widehat{\lambda}^2 + (1 + 2c_2)(1 - c_2) = 0, \qquad (20)$$

where

$$\widehat{\lambda}_1 = \frac{1}{2} \left[-4 + 2c_2 + 2\left(9c_2^2 - 8c_2\right)^{(1/2)} \right]^{(1/2)},$$

$$\widehat{\lambda}_2 = -\frac{1}{2} \left[-4 + 2c_2 + 2\left(9c_2^2 - 8c_2\right)^{(1/2)} \right]^{(1/2)},$$

$$\qquad (21)$$

$$\widehat{\lambda}_3 = \frac{1}{2} \left[-4 + 2c_2 - 2\left(9c_2^2 - 8c_2\right)^{(1/2)} \right]^{(1/2)},$$

$$\widehat{\lambda}_4 = -\frac{1}{2} \left[-4 + 2c_2 - 2\left(9c_2^2 - 8c_2\right)^{(1/2)} \right]^{(1/2)}.$$

It is noticed that $\widehat{\lambda}_1$ and $\widehat{\lambda}_2$ are two equal and opposite real roots, and $\widehat{\lambda}_3$ and $\widehat{\lambda}_4$ are a pair of pure imaginary roots. Hence, the general solution of equation (14) assumes the following form:

$$x_1 = I_1 e^{\widehat{\lambda}_1 t} + I_2 e^{-\widehat{\lambda}_2 t} + I_3 \cos(\lambda t) + I_4 \sin(\lambda t),$$

$$y_1 = -k_1 I_1 e^{\widehat{\lambda}_1 t} + k_1 I_2 e^{-\widehat{\lambda}_2 t} - k_2 I_3 \sin(\lambda t) + k_2 I_4 \cos(\lambda t),$$

$$z_1 = J_1 \cos(\omega t) + J_2 \sin(\omega t),$$

$$(22)$$

where coefficients $I_1, \ldots, I_4, k_1, k_2, J_1$ and J_2 are all constants and λ is the mould of $\widehat{\lambda}_3$ and $\widehat{\lambda}_4$.

Since the motion of the third body may be unbounded due to the influence of exponential terms, appropriate initial conditions are selected such that $I_1 = I_2 = 0$, which implies that

$$x_1 = I_3 \cos(\lambda t) + I_4 \sin(\lambda t),$$
$$y_1 = -k_2 I_3 \sin(\lambda t) + k_2 I_4 \cos(\lambda t), \qquad (23)$$
$$z_1 = J_1 \cos(\omega t) + J_2 \sin(\omega t),$$

i.e.,

$$x_1 = -A_x \cos(\lambda t + \phi),$$
$$y_1 = k_2 A_x \sin(\lambda t + \phi), \qquad (24)$$
$$z_1 = A_z \sin(\omega t + \psi),$$

where

$$A_x = \sqrt{I_3^2 + I_4^2},$$

$$A_Z = \sqrt{J_1^2 + J_2^2},$$

$$k_2 = \frac{1 + 2c_2 + \lambda^2}{2\lambda} = \frac{2\lambda}{\lambda^2 - c_2 + 1},$$

$$\cos\phi = -\frac{I_3}{A_x}, \qquad (25)$$

$$\sin\phi = \frac{I_4}{A_x},$$

$$\cos\psi = -\frac{J_2}{A_Z},$$

$$\sin\psi = \frac{J_1}{A_Z}.$$

If the value of (λ/ω) in equation (24) is an irrational number, according to the time history diagrams in Figure 2, this linearization motion of the system appears to make the periodic motion in the x and y components, respectively. However, it is not periodic but Lissajous-type quasiperiodic in the x-y plane, and this fact can be verified by the integral curves with respect to x and y (see Figure 3) and its projections in the x-y plane, as well as the portraits in the frame of x-y-z (see Figure 4). The significance of Figures 2–4 is that if the frequency of the third body in all directions is not commensurable, it will exhibit a quasiperiodic motion. Therefore, the value of (λ/ω) is a rational number that performs a critical role in the motion law of the system. In general, if the value of (λ/ω) is an irrational number, the time history diagram can only serve as a reference but a standard to judge if the system makes the periodic motion or not. On the contrary, the motion law of the system can be judged by phase portraits and time history diagrams.

In addition, note that the halo-type periodic orbits play particular importance in the actual mission ACE, ISEE-3/ICE, MAP, SOHO, Genesis, etc., that is, the in-plane and out-of-plane motion makes those characteristic frequencies equal within the sufficiently large motion region. Therefore, without loss of generality, we consider here the case of $\lambda = \omega$. Then, equation (24) can be represented as

$$x_1 = A_1(T_1)e^{i\lambda T_0} + \overline{A}_1(T_1)e^{-i\lambda T_0},$$
$$y_1 = ik_2 A_1(T_1)e^{i\lambda T_0} - ik_2\overline{A}_1(T_1)e^{-i\lambda T_0}, \qquad (26)$$
$$z_1 = A_2(T_1)e^{i\lambda T_0} + \overline{A}_2(T_1)e^{-i\lambda T_0}.$$

Substituting equation (26) into equation (15), it yields

$$D_0^2 x_2 - 2D_0 y_2 - (1 + 2c_2)x_2 + 2i\lambda D_1 A_1 e^{i\lambda T_0} - 2i\lambda D_1\overline{A}_1 e^{-i\lambda T_0} - 2ik_2 D_1 A_1 e^{i\lambda T_0} + 2ik_2 D_1\overline{A}_1 e^{-i\lambda T_0} = 0,$$
$$D_0^2 y_2 + 2D_0 x_2 + (c_2 - 1)y_2 - 2\lambda k_2 D_1 A_1 e^{i\lambda T_0} - 2\lambda k_2 D_1\overline{A}_1 e^{-i\lambda T_0} + 2D_1 A_1 e^{i\lambda T_0} + 2D_1\overline{A}_1 e^{-i\lambda T_0} = 0, \qquad (27)$$
$$D_0^2 z_2 + c_2 z_2 + 2i\lambda D_1 A_2 e^{i\lambda T_0} - 2i\lambda D_1\overline{A}_2 e^{-i\lambda T_0} = 0.$$

Let the secular term be equal to zero, and we find that

$$D_1 A_1(\lambda - k_2) = 0,$$
$$D_1 A_1(k_2 - 1) = 0, \qquad (28)$$
$$D_1 A_2 = 0.$$

Hence,

$$A_1 = \frac{\rho_1}{2},$$
$$A_2 = \frac{\rho_2}{2}, \qquad (29)$$

where ρ_1 and ρ_2 are constants.

Substituting equation (29) into equation (26), and set constant $k_2 = \delta$, we obtain

$$x_1 = \rho_1 \cos(\lambda t),$$
$$y_1 = -\delta\rho_1 \sin(\lambda t), \qquad (30)$$
$$z_1 = \rho_2 \cos(\lambda t).$$

Then, equation (27) can be expressed as

$$D_0^2 x_2 - 2D_0 y_2 - (1 + 2c_2)x_2 = 0,$$
$$D_0^2 y_2 + 2D_0 x_2 + (c_2 - 1)y_2 = 0, \qquad (31)$$
$$D_0^2 z_2 + c_2 z_2 = 0.$$

Similarly, solutions to equation (31) can be denoted as

$$x_2 = B_1(T_1)e^{i\lambda T_0} + \overline{B}_1(T_1)e^{-i\lambda T_0},$$
$$y_2 = i\delta B_1(T_1)e^{i\lambda T_0} - i\delta\overline{B}_1(T_1)e^{-i\lambda T_0}, \qquad (32)$$
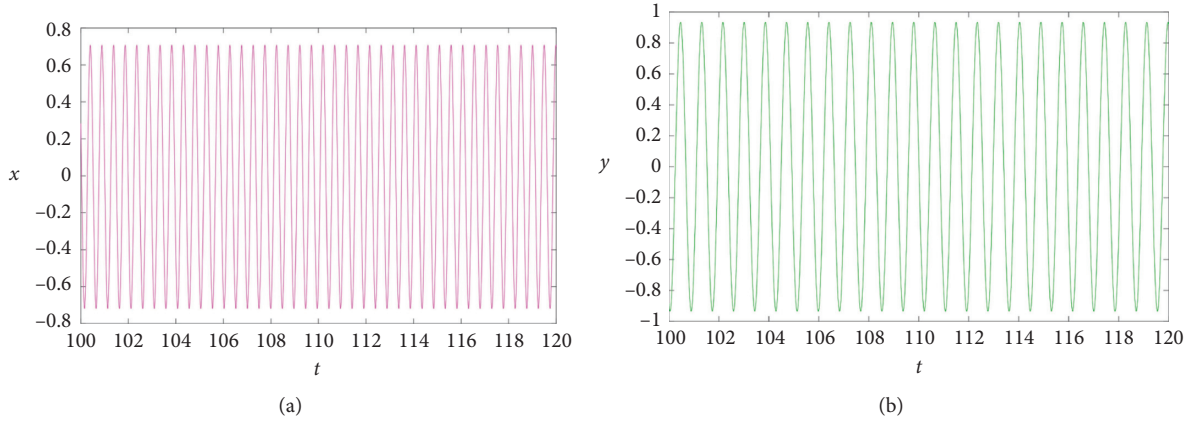$$z_2 = B_2(T_1)e^{i\lambda T_0} + \overline{B}_2(T_1)e^{-i\lambda T_0}.$$

FIGURE 2: Time history diagrams with respect to (a) x and (b) y, respectively, when $\mu = 0.0123$.
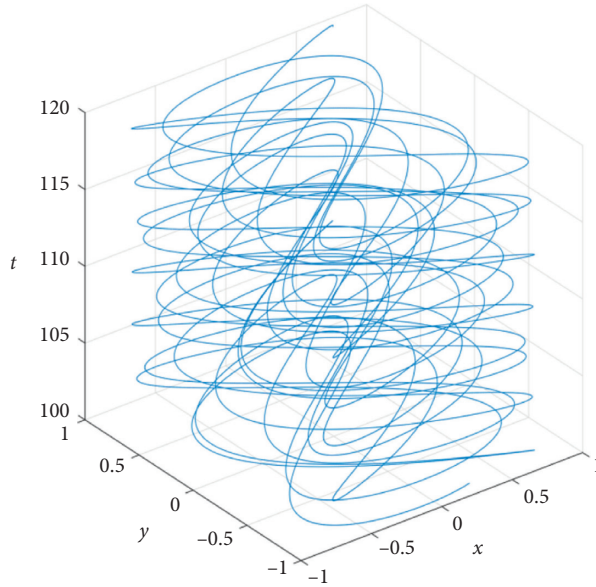

FIGURE 3: Quasiperiodic orbit of Lissajous type in x-y-t space for $\mu = 0.0123$.

Substituting equations (26) and (32) into equation (16), it yields

$$
\begin{aligned}
2i(\lambda - \delta)D_1 B_1 e^{i\lambda T_0} + 2i(\delta - \lambda)D_1 \overline{B}_1 e^{-i\lambda T_0} &= \frac{3}{4}c_3 \left[\left((2 + \delta^2)\rho_1^2 - \rho_2^2 \right)\cos(2\lambda T_0) + \left(2 - \delta^2 \right)\rho_1^2 - \rho_2^2 \right], \\
2(1 - \lambda\delta)D_1 B_1 e^{i\lambda T_0} + 2(1 - \lambda\delta)D_1 \overline{B}_1 e^{-i\lambda T_0} &= -3c_3 i\delta A_1^2 e^{i2\lambda T_0} + 3c_3 i\delta \overline{A}_1^2 e^{-i2\lambda T_0}, \\
2i\lambda D_1 B_2 e^{i\lambda T_0} - 2i\lambda D_1 \overline{B}_2 e^{-i\lambda T_0} &= -3c_3 A_1 A_2 e^{i2\lambda T_0} - 3c_3 \overline{A}_1 \overline{A}_2 e^{-i2\lambda T_0} - 3c_3 \left(A_1 \overline{A}_2 + \overline{A}_1 A_2 \right).
\end{aligned}
\tag{33}
$$

We define

(a)

(b)
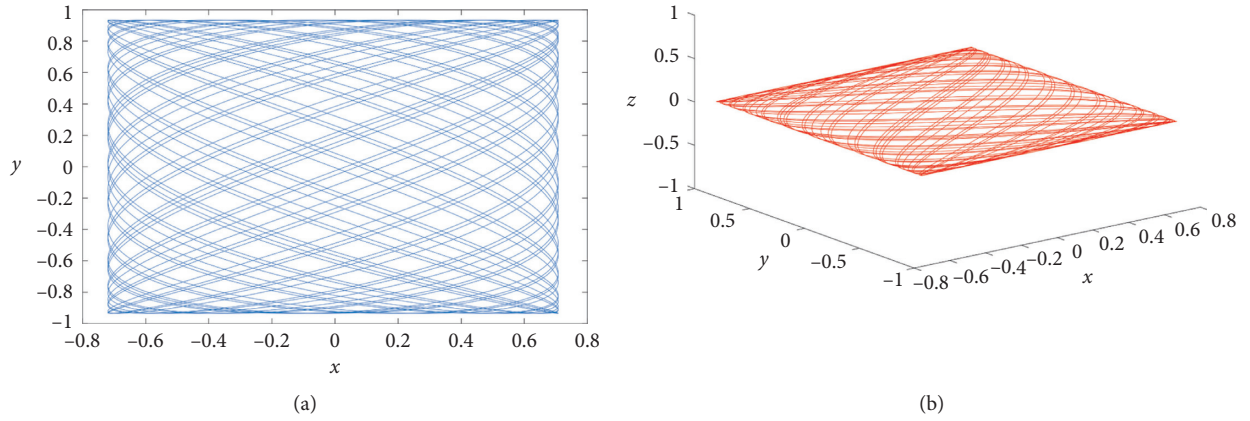
FIGURE 4: Quasiperiodic orbit of Lissajous type in the (a) x-y plane and (b) x-y-z space, respectively, when $\mu = 0.0123$.

$$B_1(T_1) = \frac{1}{2}\alpha_1(T_1)e^{i\beta_1(T_1)},$$
$$B_2(T_1) = \frac{1}{2}\alpha_2(T_1)e^{i\beta_2(T_1)}. \tag{34}$$

Thus,

$$D_1 B_1 = \frac{1}{2}\alpha_1' e^{i\beta_1} + \frac{1}{2}\alpha_1 e^{i\beta_1}(i\beta_1'),$$
$$D_1 \overline{B}_1 = \frac{1}{2}\alpha_1' e^{-i\beta_1} + \frac{1}{2}\alpha_1 e^{-i\beta_1}(-i\beta_1'),$$
$$D_1 B_2 = \frac{1}{2}\alpha_2' e^{i\beta_2} + \frac{1}{2}\alpha_1 e^{i\beta_2}(i\beta_2'),$$
$$D_1 \overline{B}_2 = \frac{1}{2}\alpha_2' e^{-i\beta_2} + \frac{1}{2}\alpha_2 e^{i\beta_2}(-i\beta_2'). \tag{35}$$

Substituting equations (35) and (30) into equation (33), we get

$$2(\lambda - \delta)\left[\alpha_1' \sin(\lambda T_0 + \beta_1) + \alpha_1 \beta_1' \cos(\lambda T_0 + \beta_1)\right] = \frac{3}{4}c_3\left[\left((2 + \delta^2)\rho_1^2 - \rho_2^2\right)\cos(2\lambda T_0) + \left(2 - \delta^2\right)\rho_1^2 - \rho_2^2\right],$$
$$2(1 - \lambda\delta)\left[\alpha_1' \cos(\lambda T_0 + \beta_1) - \alpha_1 \beta_1' \sin(\lambda T_0 + \beta_1)\right] = \frac{3}{2}c_3\delta\rho_1^2 \sin(2\lambda T_0), \tag{36}$$
$$-2\lambda\left[\alpha_2' \sin(\lambda T_0 + \beta_2) + \alpha_2 \beta_2' \cos(\lambda T_0 + \beta_2)\right] = -\frac{3}{2}c_3\delta\rho_1\rho_2\left[\cos(2\lambda T_0) + 1\right].$$

Then, it can be followed from equation (36) that

$$\alpha_1'(T_1) = \frac{3}{8(\delta - \lambda)} c_3 \left[\left(\left(2 + \delta^2 \right) \rho_1^2 - \rho_2^2 \right) \cos(2\lambda t) + \left(2 - \delta^2 \right) \rho_1^2 - \rho_2^2 \right] \sin(\lambda t + \beta_1(T_1)) + \frac{3}{4(1 - \lambda\delta)} c_3 \delta \rho_1^2 \sin(2\lambda t) \cos(\lambda t + \beta_1(T_1)),$$

$$\alpha_1 \beta_1'(T_1) = \frac{3}{8(\delta - \lambda)} c_3 \left[\left(\left(2 + \delta^2 \right) \rho_1^2 - \rho_2^2 \right) \cos(2\lambda t) + \left(2 - \delta^2 \right) \rho_1^2 - \rho_2^2 \right] \cos(\lambda t + \beta_1(T_1)) - \frac{3}{4(1 - \lambda\delta)} c_3 \delta \rho_1^2 \sin(2\lambda t) \sin(\lambda t + \beta_1(T_1)).$$

$$(37)$$

Substituting equation (34) into equation (32), we arrive at

$$\begin{aligned} x_1 &= \alpha_1(T_1) \cos(\lambda t + \beta_1(T_1)), \\ y_1 &= -\delta\alpha_1(T_1) \sin(\lambda t + \beta_1(T_1)), \\ z_1 &= \alpha_2(T_1) \cos(\lambda t + \beta_2(T_1)). \end{aligned} \quad (38)$$

Combining equations (10), (30), and (38), an approximate 3D multiple time scales solution to equation (9) can be represented as

$$\begin{aligned} x &= \varepsilon\rho_1 \cos(\lambda t) + \varepsilon^2 \cos(\lambda t + \beta_1(\varepsilon t)), \\ y &= -\varepsilon\delta\rho_1 \sin(\lambda t) - \varepsilon^2 \delta\alpha_1(\varepsilon t) \sin(\lambda t + \beta_1(\varepsilon t)), \\ z &= \varepsilon\rho_2 \cos(\lambda t) + \varepsilon^2 \alpha_2(\varepsilon t) \cos(\lambda t + \beta_2(\varepsilon t)). \end{aligned} \quad (39)$$

where α_1 and β_1 satisfy equation (37) and α_2 and β_2 satisfy the third equation of (36).

4. Conclusions

In this paper, we first show the chaotic characteristics of the classical CRTBP through the bifurcation diagram concerning the mass parameter μ, which indicates that it is challenging to find the periodic orbit by adjusting the initial conditions of the problem. The astronomer Poincaré has also shown that the probability of the event is zero. Secondly, we also show that even though sometimes the third body may exhibit corresponding periodic motions in different directions in space, the incommensurability of their frequencies will cause the third body to have quasiperiodic characteristics.

When the third body moves with a small amplitude, we construct a kind of approximate 3D multiscale solution by decomposing the conventional time contained in the solution of the CRTBP into the coupling effect of multiple time scales. The shortcoming of this type of solution is that, like other known approximate solutions (such as those based on the Lindstedt–Poincaré method), the result of error analysis is not satisfactory because of the chaotic nature of the problem. In theory, we need more infinite terms in solution series and time scales to make it approach the exact solution of the problem, but this is worthless, and the analytical calculation under the current technological level is almost impossible to achieve. Therefore, we only need the series approximation of two or three terms, so that the multiple time scales solution can be used as an initial guess or approximation of the low-energy transfer orbital mission (such as Genesis discovery mission), and then generate spacecraft orbit through some differential correction procedures. In addition, the classic ISEE-3 mission actually used a similarly constructed approximate solution as the initial solution for orbit design.

Data Availability

No data were used to support this study.

Conflicts of Interest

The authors declare that they have no conflicts of interest.

Acknowledgments

References

[1] J. L. Zhou and Y. S. Sun, *Celestial Mechanics: A Story From an Apple/10000 Selected Problems in Sciences*, Astronomy Volume, Science Press, Beijing, China, 2010, in Chinese.

[2] R. W. Farquhar and A. A. Kamel, "Quasi-periodic orbits about the translunar libration point," *Celestial Mechanics*, vol. 7, pp. 458–473, 1973.

[3] D. L. Richardson, "Halo orbit formulation for the ISEE-3 mission," *Journal of Guidance and Control*, vol. 3, pp. 543–548, 1980.

[4] D. L. Richardson, "Analytical construction of periodic orbits about the collinear points," *Celestial Mechanics*, vol. 22, pp. 241–253, 1980.

[5] T. W. Ruijgrok, "The exact solution of a three-body problem," *European Journal of Physics*, vol. 5, pp. 21–24, 1984.

[6] C. Zagouras and V. V. Markellos, "Three-dimensional periodic solutions around equilibrium points in hill's problem," *Celestial Mechanics*, vol. 35, pp. 257–267, 1985.

[7] K. Papadakis, E. Perdios, and V. V. Markellos, "Nonlinear approximation of periodic three-body motions around collinear equilibrium configurations," *Astrophysics and Space Science*, vol. 140, pp. 373–383, 1988.

[8] G. Gómez, J. J. Masdemont, and C. Simó, "Quasihalo orbits associated with libration points," *The Journal of the Astronautical Sciences*, vol. 46, pp. 135–176, 1998.

[9] S. T. Lu and Y. S. Zhao, "The improvement of Richardson's three order approximate analytical solution of halo orbit," *Journal of Astronautics*, vol. 30, pp. 863–869, 2009, (in Chinese).

[10] M. Gidea and F. Deppe, "Chaotic orbits in a restricted three-body problem: numerical experiments and heuristics," *Communications in Nonlinear Science and Numerical Simulation*, vol. 11, pp. 161–171, 2006.

[11] M. Suvakov and V. Dmitrasinovic, "Three classes of Newtonian three-body planar periodic orbits," *Physical Review Letters*, vol. 110, Article ID 114301, 2013.

[12] A. Mittal, M. S. Suraj, and R. Aggarwal, "The analysis of periodic orbits generated by lagrangian solutions of the restricted three-body problem with non-spherical primaries," *New Astronomy*, vol. 74, Article ID 101287, 2020.

[13] N. Pathak, E. I. Abouelmagd, and V. O. Thomas, "On higher order resonant periodic orbits in the photo-gravitational planar restricted three-body problem with oblateness," *The Journal of the Astronautical Sciences*, vol. 66, pp. 475–505, 2019.

[14] E. I. Abouelmagd, M. E. Awad, E. M. A. Elzayat, and I. A. Abbas, "Reduction the secular solution to periodic solution in the generalized restricted three-body problem," *Astrophysics and Space Science*, vol. 350, pp. 495–505, 2014.

[15] E. I. Abouelmagd and J. L. G. Guirao, "Periodic and secular solutions in the restricted three-body problem under the effect of zonal harmonic parameters," *Applied Mathematics & Information Sciences*, vol. 9, no. 4, pp. 1659–1669, 2015.

[16] H. H. Selim, J. L. G. Guirao, and E. I. Abouelmagd, "Libration points in the restricted three-body problem: Euler angles, existence and stability," *Discrete and Continuous Dynamical Systems Series S*, vol. 12, no. 5, pp. 703–710, 2019.

[17] F. B. Gao and Y. Q. Wang, "Approximate analytical periodic solutions to the restricted three-body problem with perturbation, oblateness, radiation and varying mass," *Universe*, vol. 6, no. 8, p. 110, 2020.

[18] F. B. Gao and R. F. Wang, "Bifurcation analysis and periodic solutions of the HD 191408 system with triaxial and radiative perturbations," *Universe*, vol. 6, no. 2, p. 35, 2020.

[19] A. H. Nayfeh, "Three-to-one resonances near the equilateral libration points," *AIAA Journal*, vol. 8, pp. 2245–2251, 1970.

[20] A. H. Nayfeh, "Two-to-one resonances near the equilateral libration points," *AIAA Journal*, vol. 9, pp. 23–27, 1971.

[21] A. H. Nayfeh and D. T. Mook, *Nonlinear Oscillations*, Wiley-Vch Verlag GmbH & Co. KGaA, Hoboken, NJ, USA, 2004.

[22] W. S. Koon, M. W. Lo, J. E. Marsden, and S. D. Ross, *Dynamical Systems, the Three-Body Problem and Space Mission Design*, Marsden Books, Wellington, New Zealand, 2011.